Application Note

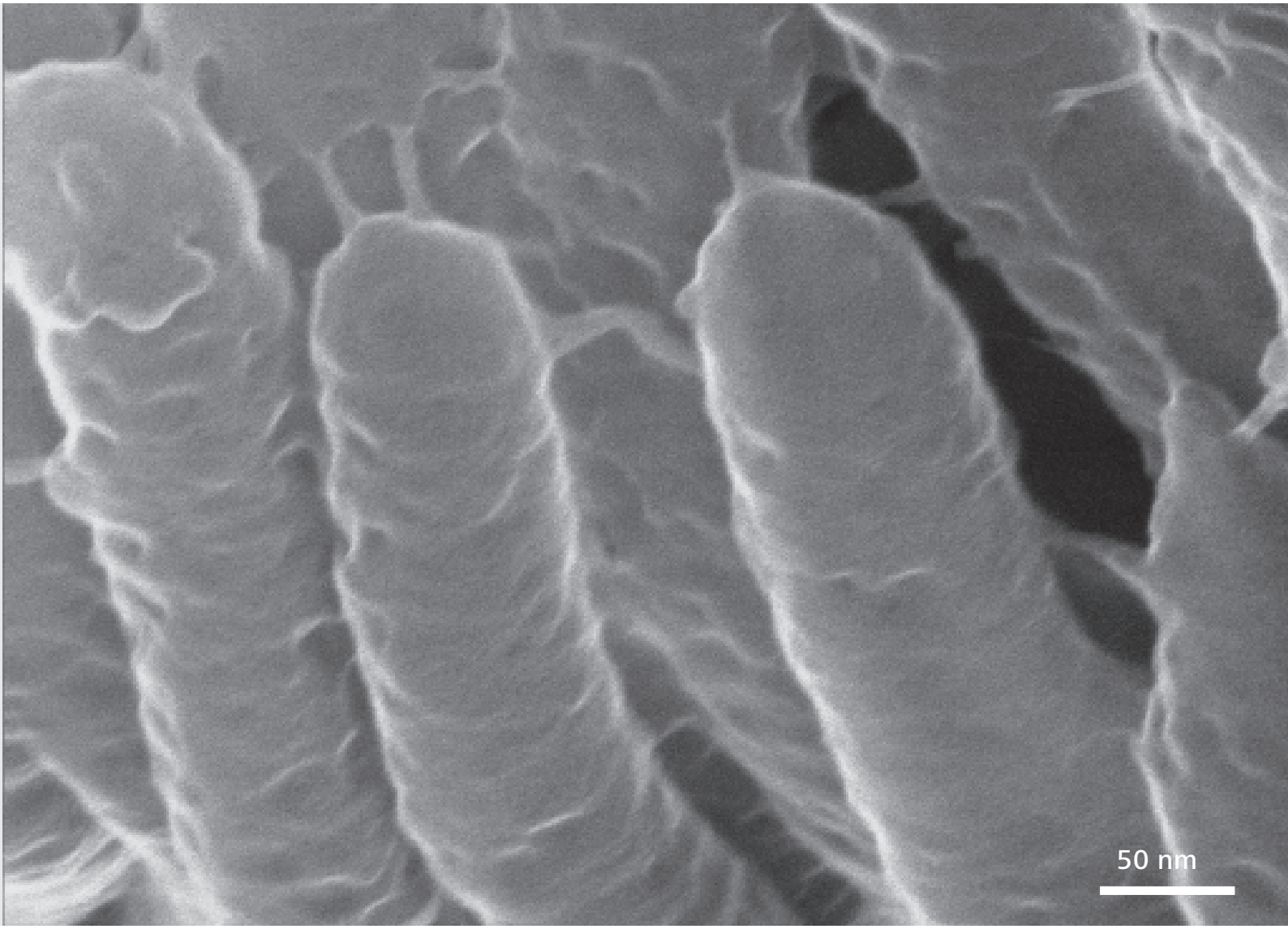

Benefits of ZEISS ORION NanoFab for High Resolution Imaging

Benefits of ZEISS ORION NanoFab for High Resolution Imaging

Date: May 2019

ZEISS ORION NanoFab leverages multiple ion beams for imaging and fabrication tasks. High resolution imaging is one of the most important techniques used to characterize a sample, and many different microscopy solutions exist to provide users with different information about a sample. This note presents application results targeting three particular benefits of ORION NanoFab. These are: high resolution imaging of nanoscale features, surface sensitive imaging of 2D materials, and easy insulator imaging, including biological samples.

Introduction

Due to the unique interaction of the helium ion beam and the sample, the image contrast mechanism with ZEISS ORION NanoFab is different from scanning electron microscopes and provides unique material contrast and enhanced surface contrast. The rich contrast and ultra-small ion beam probe size makes ORION NanoFab a powerful imaging tool for ultra-high imaging resolution, even for insulating samples, to reveal topographic, compositional, and other types of information about the specimen.

ORION NanoFab is an ideal imaging tool for surface characterization due to its ultra-high spatial resolution, great surface sensitivity, low background noise and easy charge neutralization. Researchers have demonstrated the benefits of using the helium ion beam to gain abundant surface information of 2D nanomaterials, such as graphene. ORION NanoFab provides an easy and effective way of charge neutralization, allowing it to image even insulating samples at very high resolution without the need for low vacuum techniques or conductive coatings. This significantly reduces the complexity of sample preparation and improves image fidelity without artifacts introduced from the preparation and coating.

ORION NanoFab enables helium ion microscopy (HIM), an imaging technique with high resolution, strong contrast, surface sensitivity, and no charging artifacts.

Imaging Benefit #1: Overcoming the Challenges of Imaging Nanostructures at Ultra-high Resolution with HIM

In order to see more details and nanoscale structures on biological samples, nanomaterials and advanced semiconductor circuits, a better imaging resolution is desired. Scanning electron microscopes (SEM) are widely used for imaging nanostructures; however, the image resolution is limited by the beam probe size, source brightness and the interaction volume of the beam and the sample.

It has been demonstrated that ORION NanoFab can achieve ultrahigh image resolution with probe sizes of down to 0.25 nm. A high-resolution image of asbestos fibers on holey carbon grid with a spatial resolutions of 0.25 nm at 35 kV accelerating voltage using the helium ion beam (HIM) is shown (Figure 1a). An edge finding algorithm is used to analyze this image and calculate the resolution by measuring the 25 – 75 percent rise distance across multiple edges. To our knowledge, this is the best spatial resolution in secondary electron (SE) imaging. Material and surface contrast also contribute to the imaging resolution. For different materials at different beam conditions, the resolution may or may not show the same level of resolution. For example, the resolution for the gold-on-carbon standard sample (Figure 1b) is 0.4 nm, which is still remarkable compared to commercially available SEM.

Application Example: High-resolution Images Of Biological Samples

Stereocilia of the inner ear hair cells are connected to each other by tip links. The studies of mechanoelectrical transduction (MET) in hair cells reveal that tip links play a critical role in MET. Here a stereocilia sample was imaged using both SEM and HIM to compare the effects of imaging a biological sample at high magnification. The HIM image (Figure 2b) has better surface contrast and imaging resolution to discern the size of tip links (~ 5 nm) between stereocilia compared to the SEM image (Figure 2a). The imaging resolution of SEM and HIM is 1.5 nm and 0.8 nm, respectively. It is noteworthy that the helium ion beam provides excellent contrast even for low-atomic number samples, such as carbon.

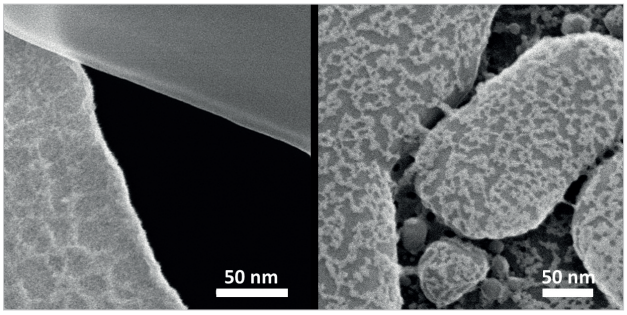

Figure 1 *(left) High resolution images of the edge of an asbestos (crocidolite) fiber resting on a holey carbon grid (right). Gold-on-carbon standard, imaged using the helium ion beam. Operation conditions: HIM: 35kV, 0.1-0.2 pA.*

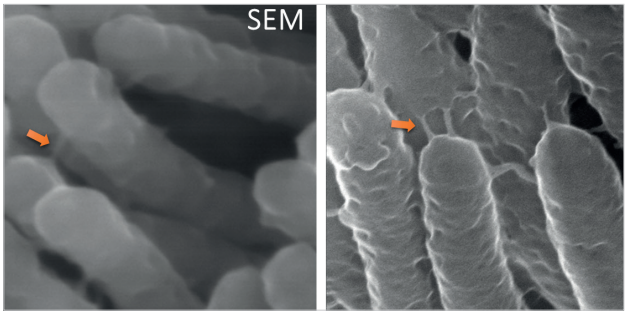

Figure 2 *(left) High-magnification images of the stereocilia from the inner ear using SEM (right). High-magnification images of the stereocilia from the inner ear using HIM. Operation conditions: SEM: 5 keV; HIM 35 kV.*

Application Example: Organic Photovoltaic (OPV) Cell Blends

The most efficient OPVs are blends of electron donating semiconductors (typically conjugated polymers) and electron acceptors (typically functionalized fullerenes). Resolving nanostructures in the OPV thin film is always challenging. Atomic Force Microscopy (AFM) scanning is a popular method for OPV thin film characterization, however scanning is time consuming and contamination on the AFM tip may introduce artificial surface information.

The helium ion beam has been demonstrated to image nanoscale thin-film blends relevant to organic opto-electronic devices and its suitability of imaging thin-films of poly (3-hexylthiophene)/[6,6]-phenyl-C61-butric acid methyl ester (P3HT/PCBM) blends has been shown. Comparative high resolution images of the OPV film by HIM and AFM after plasma cleaning are shown (Figure 3). The absence of a correlation between height variation in AFM and features in HIM image suggests the HIM image conveys primarily material contrast. The bright areas observed in HIM are P3HT-rich and the dark areas are predominantly PCBM.

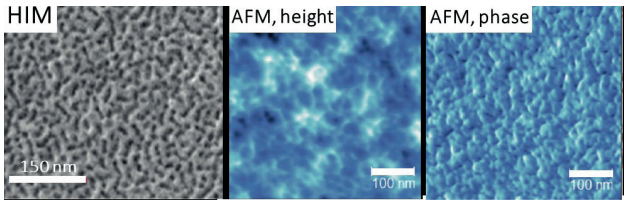

Figure 3 *(left) HIM image (middle) AFM image of height (right) AFM image of a phase-separated domain structure [1]. Operation conditions: HIM: 35 kV, 0.3-0.4 pA. The polymer thin film was cleaned using a plasma cleaner at the load-lock of ORION NanoFab.*

Advantages of the Helium Ion Beam for High-resolution Imaging

The two key attributes of the image resolution are the ion beam species and the nature of the beam interaction with the sample. Gas field ion source (GFIS) technology, special ORION source formation process, and electrostatic ion optical column design allow ORION NanoFab to have an extremely focused ion beam with a focused probe size of less than 0.5 nm and ultra-high brightness (> $5x10^9$ A/cm^{2}sr).

The interaction of the moderate energy helium ions with the sample yield images with unique material contrast and high surface sensitivity. A helium ion striking the sample produces about five times more secondary electrons (SE) than a typical scanning electron microscope at similar beam conditions. The secondary yield increases with atomic number in SEM, but is more consistent in HIM, which makes helium ion microscopy an ideal technique for imaging low-atomic number samples, such as carbon.

In this application, ORION NanoFab generates high resolution HIM images which provide compositional information about thin film photovoltaics.

Imaging Benefit #2: Imaging of 2D Materials with High Surface Sensitivity

2D materials, such as graphene and transition metal dichalcogenides (TMDs) are emerging as new materials due to their special electronic properties. The number of layers, the size of the flakes, surface contamination, deformations, and the presence of defects can significantly affect these materials' properties. However, by conventional techniques, it is quite challenging to image layers that might be less than a few atoms thick. The thin graphene sheet is almost transparent to high energy electron beams and generating sufficient secondary electrons (SE) is difficult with scanning electron microscopes. It becomes even more challenging when the surface defects are at the sub-nanometer scale. Imaging graphene at a low beam voltage can enhance the contrast in the SEM, but this comes at the expense of reducing the imaging resolution.

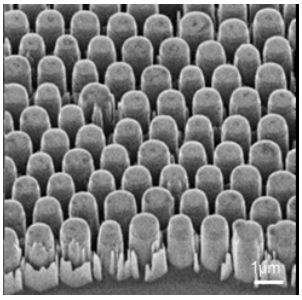

Figure 4 *Single sheet of graphene supported by gallium nitride (GaN) pillars. Operation conditions: HIM: 20-35 keV and 0.1 pA to 1.5 pA. Image courtesy of: M. Latzel, M. Heilmann, G. Sarau, S.H. Christiansen, Max Planck Institute for the Science of Light, Erlangen, Germany.*

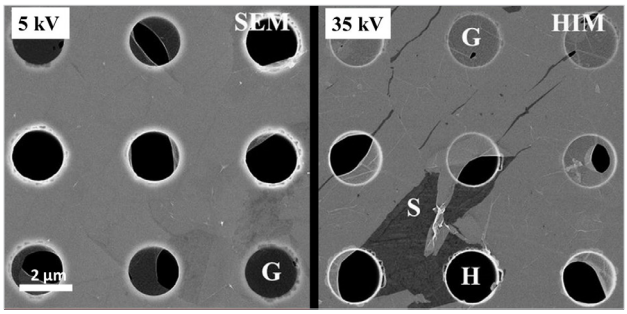

Figure 5 *Low-magnification images of different regions of the graphene sample observed using SEM (left) and HIM (right) [2]. Both the images have the same field of view. Operation conditions: SEM: 5 keV; HIM 35 kV.*

Application Example: Graphene Characterization

ORION NanoFab has been employed to characterize 2D nanomaterials because of its high resolution and surface sensitive imaging capability. A graphene thin sheet on gallium nitride pillars in HIM is abundant with surface details, such as holes, ruptures, multilayer folds and ridges (Figure 4).

The comparison of SEM and HIM images of a free-standing graphene across the substrate holes is also shown (Figure 5). The existence of graphene (marked as "G" in the image) can be identified from the substrate "S" and the bare holes "H". The graphene has a better contrast in HIM compared to SEM. The contrast of graphene on the substrate is distinguishable in the HIM image, but difficult to identify in the SEM image at the selected magnification.

ORION NanoFab has also been able to distinguish between mono- and multilayers of graphene flakes by the difference in which the SE intensity is reduced with increasing layer thickness. The HIM image can clearly discern the graphene sample at least up to 7 layers (Figure 6). Line-scan profile of a HIM image also shows the layer dependence of graphene SE contrast, with precisely defined edges. The SE intensity in SEM has the similar trend [4], but the contrast is less sensitive than the SE contrast in HIM. It becomes difficult to use SEM to distinguish the 3rd or 4th layer (marked with the green arrows in the plot).

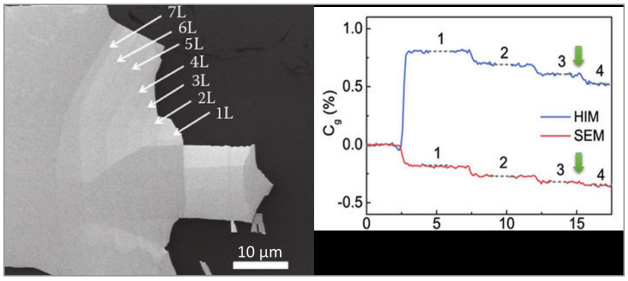

Figure 6 *(left) A typical HIM image of a piece of mechanically exfoliated graphene flake with regions of different thickness on a SiO_2/Si substrate. (right) Line profiles of SE contrast for the 1~4 layer graphene.*

Advantages of the Helium Ion Beam for 2D Nanomaterials Imaging

Images acquired in the ORION NanoFab are formed by collecting secondary electrons (SE) generated during the interaction between the sample and the primary helium ion beam. Due to the highly localized interaction of helium ions in a sample, and lower energies of the SE, HIM images show greater surface details (topographical contrast) than conventional SEM at equivalent acceleration voltages. For example, at a typical HIM acceleration voltage of 30 kV only secondary electrons produced from the top few nanometers of a sample can reach the detector and therefore generate very surface sensitive images.

The primary helium ion beam also has a low backscatter probability, so SE1 electrons are the main signal produced by the helium ion beam. The subsurface and peripheral information is supressed resulting in the highest resolution and enhanced material contrast over SEM imaging.

Due to the stronger dependence of SE yield on the helium ion incidence angle than the electron incidence angle in the SEM, the HIM images show greater edge contrast of nanomaterials profiles than the SEM at equivalent acceleration voltages.

In summary, ORION NanoFab is an ideal imaging tool to image very thin nanosheets and provide rich surface details, such as surface morphology, layer numbers, layer edge, surface defects, graphene folds, and surface contaminations due to its unique sample interaction.

Imaging Benefit #3: Charge Control for Imaging Insulating Samples

Conventional secondary electron microscopes (SEM) can image conductive samples with high resolution, but non-conductive samples remain a challenge. Charge can easily build up on the surface of non-conductive samples, distorting the images, reducing contrast, lessening image resolution, and even causing sample damage through dielectric breakdown. Very often a conductive coating is applied prior to imaging; however, this may destroy or, at the very least, obscure fine surface details. Another way to reduce the charging effect is to lower the accelerating voltage which decreases image resolution.

Application Example: Low-k Semiconductor Samples

Imaging of nanoscale features in low-k or ultra-low-k dielectric materials is important for interconnect validation. Due to the electron beam irradiation damage, the line width, shape and surface roughness of low-k materials are often changed by SEM imaging. Since these materials are non-conducting, a low accelerating voltage is typically used to minimize charging effects, which however compromises contrast and resolution. Charging in ORION NanoFab is controlled and mitigated by means of a chamber-mounted electron flood gun. High resolution images of low-k dielectric lines and spaces using SEM and the helium ion microscope [5] are shown (Figure 7). The helium ion image clearly shows higher resolution and contrast and allows for the measurement of surface and side wall roughness with high precision.

Application Example: Pore Networks within Shale and Coal

Pore size distribution and structure contribute significantly to storage volume and transport pathways within shale resource rocks. The pore diameters can range from hundreds of microns to nanometers, and they can form a connected network, or be isolated. These characteristics determine the likelihood that gas will accumulate, which is a key factor in assessing the energy content of this natural resource. Evaluation requires versatile and advanced imaging capabilities. [6] [7] [8].

In addition, shales are very prone to charging due to variable mineral size, clay particles, organic phases, and the interaction of minerals. Using a conventional SEM with a lower accelerating voltage for rough and uncoated surfaces can help reduce the charging effect, but this approach sacrifices imaging resolution. ORION NanoFab on the other hand combines ultra-high resolution (probe size <0.5 nm) and a large depth of field with a low energy electron flood gun to neutralize charge, which allows to accurately measure pore size and distribution.

A Bossier shale sample was imaged in both a SEM and HIM using the same field of view (Figure 8). The helium ion image clearly shows reduced charging artifacts, higher resolution, and better contrast. Even fine structures within the pores are resolved. Furthermore, it was reported that the increased depth of field in HIM images compared to SEM can remove the need to acquire 3-dimensional SEM datasets using FIB-SEM [9].

Application Example: Biological Samples

Many microbiological samples have been imaged using helium ion microscopy, for example mammalian cells, such as human colon cancer cells [10], human liver cells [11], rabbit cartilage collagen networks [12], HeLa cells [13], rat kidney [14], rat and mouse epidermis [15], and human neural stem cells, neurons, and mouse neurons [16]. HIM has been also used to image scales of lepidoptera (butterfly) wings [17], sea corals [18] and cuticle structures in *Drosophila* [19]. Recently, microbial interaction between bacteria [20] and their viruses has been studied using HIM [21]. Many of these studies have shown that uncoated samples reveal a finer ultrastructure than coated samples.

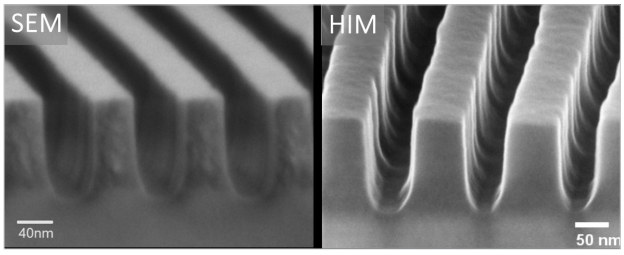

Figure 7 *(left) High resolution images of low-k dielectric lines and spaces using SEM (right) same areas observed in HIM. Operating conditions: HIM: 35 kV, 0.1-0.2 pA.*

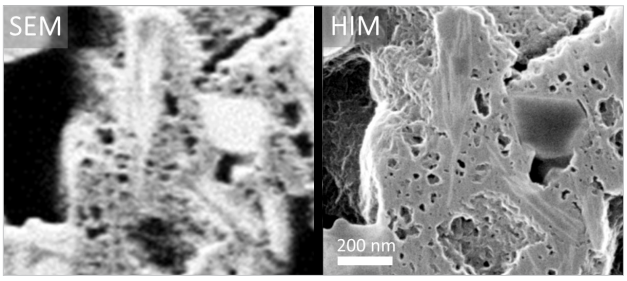

Figure 8 *(left) SEM image of a Bossier shale sample (right) same area observed in a HIM. Operating conditions: SEM: 1 keV accelerating voltage with 10 nm pixel size; HIM 30 keV with 1.2 nm pixel size.*

Examples of imaging biological samples with SEM compared to HIM are shown (Figure 9). Since the samples were critical point dried and uncoated, they were prone to charging and thus low voltage (0.7 - 1 kV) imaging in the FE-SEM was used. However, the sample still exhibited charging effects at high magnification and no fine structure can be discerned. In contrast, charging in the HIM was completely mitigated using an electron flood gun. As a result, higher magnifications could be easily achieved without any form of charging, thermal drift and most importantly beam-induced damage, thus clearly revealing fine surface structures.

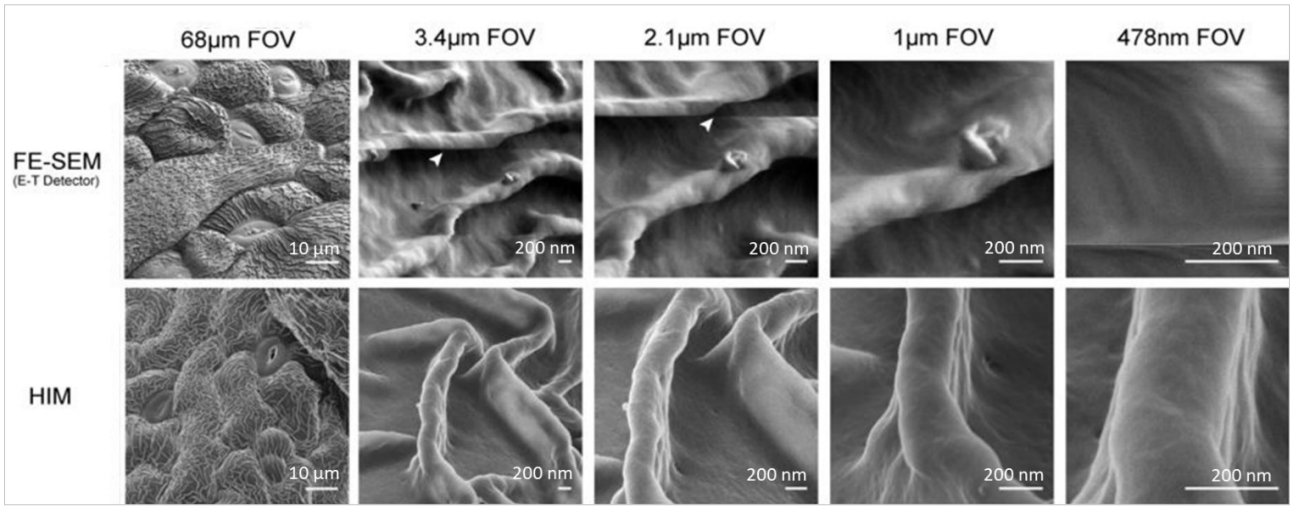

Figure 9 Low and high magnification series of uncoated and critical point dried Arabidopsis thaliana sepal cuticle structures in the FE-SEM at low voltage and HIM. Charging artifacts become visible in FE-SEM in the form of streaks or bands (white arrow). Image Courtesy of National Institutes of Health.

Advantages of The Helium Ion Beam to Image Insulating Samples

Easy charge neutralization: The electron flood gun in the ORION NanoFab provides low energy electrons around the image field to neutralize the positively charged area created by the helium ion beam. This charge neutralization enables the ORION NanoFab to maintain charge balance and produce high-resolution images and detailed surface information with high fidelity.

High SE yield: It is worth emphasizing the high secondary electron (SE) yield induced by helium ion beam allowing imaging with low beam currents. This creates a steady charge state and stable imaging with less charge built up.

Simple sample preparation: Due to the easy charge neutralization method there is no need to add additional conductive coating on insulting samples.

High image fidelity: Unlike SEMs, there is no need for an additional conductive coating on insulating samples. This significantly improves image fidelity without artifacts introduced from the preparation and additional coatings.

In summary, ORION NanoFab is an ideal instrument for imaging insulating samples. A few application examples are listed above, such as low-k semiconductors, shale and coals, and biological samples. Easy charge neutralization, high SE yield, simple sample preparation and high image fidelity are the main advantages helium ion imaging has over conventional SEMs.

References:

[1] A.J. Pearson, S.A. Boden, D.M. Bagnall, D.G. Lidzey, and C. Rodenburg, "Imaging the Bulk Nanoscale Morphology of Organic Solar Cell Blends Using Helium Ion Microscopy," Nano Letters, Vol. 11(10), pp. 4275–4281, (2011).

[2] Y. Zhou, R. O'Connell, P. Maguire, and H. Zhang, "High Throughput Secondary Electron Imaging of Organic Residues on a Graphene Surface", Scientific Reports, Vol. 4, 7032, (2014).

[3] Y. Zhou, D.S. Fox, P. Maguire, R. O'Connell, R. Masters, C. Rodenberg, H. Wu, M. Dapor, Y. Chen, H. Zhang, "Quantitative Secondary Electron Imaging for Work Function Extraction at Atomic Level and Layer Identification of Graphene," Scientific Reports, Vol. 6, 21045, (2016).

[4] D. Fox D, Y. Zhou, and H. Zhang, "Chapter 8: Helium Ion Microscopy for Graphene Characterization and Modification," in Nanotubes and Nanosheets: Functionaliza-tion and Applications of Boron Nitride and Other Nanomaterials, Taylor and Francis, (2015).

[5] S. Ogawa, W. Thompson, L. Stern, L. Scipioni, J. Notte, L. Farkas, and L. Barriss, "Helium Ion Secondary Elecron Mode Microscopy for Interconnect Material Imaging," Japanese Journal of Applied Physics, Vol. 49 (4S), 04DB12-1, (2010).

[6] H.E. King Jr., APR Eberle, C.C. Walters, C.E. Kliewer, D. Ertas, and C. Huynh, "Pore Architecture and Connectivity in Gas Shale," Energy Fuels, Vol. 29(3), pp. 1375-1390, (2015).

[7] X. Tang, Z. Jiang, S. Jiang, P. Wang, and C. Xiang, "Effect of Organic Matter and Maturity on Pore Size Distribution and Gas Storage Capacity in High-Mature to Post-Mature Shales," Energy Fuels, Vol. 30(11), pp. 8985-8996, (2016).

[8] T. Cavanaugh, J. Walls, "Multi-Resolution Imaging of Shales Using Electron and Helium Ion Microscopy", https://timothycavanaugh.files.wordpress.com/2015/07/imaging-of-shales-using-electron-and-ion-microscopy.pdf, accessed 21 May 2019.

[9] C.C. Walters and C.E. Kliewer, "Helium Ion Microscopy - Geologic Applications," as presented at the Goldschmidt Conference, Sacramento, California, June 8-13, (2014).

[10] D. Bazou, G. Behan, C. Reid, J.J. Boland, and H.Z. Zhang, "Imaging of Human Coon Cancer Cells Using He-Ion Scanning Microscopy," Journal of Microscopy, Vol. 242(3), pp. 290-294, (2011).

[11] X. Chen, C.N.B. Udalagama, C-B. Chen, A.A. Bettiol, D.S. Pickard, T. Venkatesan, and F. Watt, "Whole-Cell Imaging at Nanometer Resolutions Using Fast and Slow Focused Helium Ions," Biophysical Journal, Vol. 101(7), pp. 1788-1793, (2011).

[12] W.S. Vanden Berg-Foels, L. Scipioni, C. Huynh, and X. Wen, "Helium Ion Microscopy for High-Resolution Visualization of the Articular Cartilage Collagen Network," Journal of Microscopy, Vol. 246(2), pp. 168-176 (2012).

[13] M.S. Joens, C. Huynh, J.M. Kasuboski, D. Ferranti, Y.J. Sigal, F. Zeitvogel, M. Obst, C.J. Burkhardt, K.P. Curran, S.H. Chalsasani, L.A> Stern, B. Goetze, and J.A.J. Fitzpatrick, "Helium Ion Microscopy (HIM) for the Imaging of Biological Samples at Sub-Nanometer Resolution," Scientific Reports, Vol. 3, p.3514, (2013).

[14] W.L. Rice, A.N. Van Hoek, T.G. Păunescu, C. Huynh, B. Goetze, B. Singh, L. Scipioni, L.A. Stern, D. Brown, "High Resolution Helium Ion Scanning Microscopy of the Rat Kidney," PLoS ONE, Vol. 8(3), e57051 (2013).

[15] T.G. Păunescu, W.W.C. Shum, C. Huynh, L. Lechner, B. Goetze, D. Brown, and S. Breton, "High-Resolution Helium Ion Microscopy of Epididymal Epithelial Cells and their Interaction with Spermatozoa," Molecular Human Reproduction, Vol. 20(10), pp. 929-937, (2014).

[16] M. Schürmann, N. Frese, A. Beyer, P. Heimann, D. Widera, V. Mönkemöller, T. Huser, B. Kaltschmidt, C. Kaltschmidt, and A. Gölzhäuser, "Helium Ion Microscopy Visualizes Lipid Nanodomains in Mammalian Cells," Small, Vol. 11(43), pp. 5781-5789, (2015).

[17] S.A. Boden, A. Asadollahbaik, H.N. Rutt, D.M. Bagnall, "Helium Ion Microscopy of Lepidoptera Scales," Scanning Vol. 34(2), pp. 107-120, (2012).

[18] Biological control of aragonite formation in stony corals. Stanislas Von Euw, Qihong Zhang, Viacheslav Manichev, Nagarajan Murali, Juliane Gross, Leonard Feldman, et al. Science: Vol. 356, Issue 6341, (2017) pp. 933-938

[19] A. Boseman, K. Nowlin, S. Ashraf, J. Yang, D. Lajeunesse, "Ultrastructural Analysis of Wild Type and Mutant Drosophila Melanogaster Using Helium Ion Microscopy," Micron Vol. 51, pp. 26-35 (2013).

[20] N. Said, A. Chatzinotas, and M. Schmidt, "Have an Ion on It: The Life-Cycle of Bdellovibrio Bacteriovorus Viewed by Helium-Ion Microscopy," Advanced Biosystems, Vol. 3(1): 1800250, (2018).

[21] M. Leppänen, L.-R. Sundberg, E. Laanto, G.M. de Freitas Almeida, P. Papponen I.J. Maasilta, "Bioimaging: Imaging Bacterial Colonies and Phage–Bacterium Interaction at Sub-Nanometer Resolution Using Helium-Ion Microscopy," Advanced Biosystems, Vol. 1(8): 1700070, (2017).

Carl Zeiss Microscopy GmbH
07745 Jena, Germany
microscopy@zeiss.com
www.zeiss.com/microscopy